Small RNA combination therapy for lung cancer

Wen Xue[a,b,c,1], James E. Dahlman[a,d,1], Tuomas Tammela[a,b,c], Omar F. Khan[a,e], Sabina Sood[a,b,c], Apeksha Dave[a,b], Wenxin Cai[a,b,c], Leilani M. Chirino[a,b,c], Gillian R. Yang[a,b], Roderick Bronson[f], Denise G. Crowley[a,b,c], Gaurav Sahay[a], Avi Schroeder[a,g], Robert Langer[a,d,e], Daniel G. Anderson[a,d,e,2], and Tyler Jacks[a,b,c,2]

[a]David H. Koch Institute for Integrative Cancer Research, Massachusetts Institute of Technology, Cambridge, MA 02139; Departments of [b]Biology and [e]Chemical Engineering, Massachusetts Institute of Technology, Cambridge, MA 02139; [c]Howard Hughes Medical Institute, Massachusetts Institute of Technology, Cambridge, MA 02139; [d]Harvard-MIT Division of Health Sciences and Technology, Institute for Medical Engineering and Science, Massachusetts Institute of Technology, Cambridge, MA 02139; [f]Tufts University and Harvard Medical School, Boston, MA 02115; and [g]Department of Chemical Engineering, Technion-Israel Institute of Technology, Haifa 32000, Israel

Contributed by Tyler Jacks, July 8, 2014 (sent for review May 16, 2014)

MicroRNAs (miRNAs) and siRNAs have enormous potential as cancer therapeutics, but their effective delivery to most solid tumors has been difficult. Here, we show that a new lung-targeting nanoparticle is capable of delivering miRNA mimics and siRNAs to lung adenocarcinoma cells in vitro and to tumors in a genetically engineered mouse model of lung cancer based on activation of oncogenic Kirsten rat sarcoma viral oncogene homolog (*Kras*) and loss of p53 function. Therapeutic delivery of miR-34a, a p53-regulated tumor suppressor miRNA, restored miR-34a levels in lung tumors, specifically down-regulated miR-34a target genes, and slowed tumor growth. The delivery of siRNAs targeting *Kras* reduced *Kras* gene expression and MAPK signaling, increased apoptosis, and inhibited tumor growth. The combination of miR-34a and siRNA targeting Kras improved therapeutic responses over those observed with either small RNA alone, leading to tumor regression. Furthermore, nanoparticle-mediated small RNA delivery plus conventional, cisplatin-based chemotherapy prolonged survival in this model compared with chemotherapy alone. These findings demonstrate that RNA combination therapy is possible in an autochthonous model of lung cancer and provide preclinical support for the use of small RNA therapies in patients who have cancer.

miR-34 | nanotechnology

MicroRNAs (miRNAs) mediate multiple biological processes, and alterations in miRNA function have been associated with different diseases, including cancer (1–4). In model systems, the overexpression of tumor suppressor miRNAs or inhibition of oncogenic miRNAs has shown therapeutic potential (5). Moreover, siRNAs hold great promise as therapeutic agents for cancer through RNAi of oncogene expression (6–9). Although numerous studies have evaluated small RNA therapy mediated by delivery vehicles in xenograft models of cancer (5, 6, 9, 10), the relevance of these results is limited by the fact that tumors are implanted in ectopic sites. Similarly, although viral-mediated small RNA delivery has led to promising antitumor responses in genetically engineered mouse models of cancer (11, 12), the utility of viral delivery systems may be limited by preexisting immunity, toxicity, concerns about mutational genomic insertions, and insufficient delivery efficiency. To overcome these barriers, many nonviral small RNA delivery vehicles have been designed (13). Although most of these delivery vehicles have been tested in xenograft models (14, 15), some have been evaluated in autochthonous mouse models as well (16, 17).

Lung cancer is an attractive cancer type for local or systemic small RNA delivery treatment (7). It is the leading cause of cancer death worldwide, with non-small cell lung cancers (NSCLCs) accounting for 85% of all lung cancer cases (18). The most common NSCLC subtype, adenocarcinoma, is associated with frequent mutations in *KRAS* (~20–30%) and *TP53* (~50%) (18). Targeted mutations of these two genes in the adult murine lung epithelium results in lung adenocarcinomas that mimic the histopathological progression of the human disease (19). The so-called "KP" model of lung adenocarcinoma involves activation of an oncogenic *Kras* allele ($Kras^{G12D}$) and inactivation of two conditional (floxed) alleles of *p53* following intranasal or intratracheal administration of recombinant virus particles expressing Cre recombinase (19). Although lung cancers in the KP model respond to certain chemotherapeutics, durable responses have not been observed (20–25). Of note, despite recent progress in the treatment of human lung cancer carrying activating mutations in *EGFR* and translocations involving *ALK* with targeted anticancer agents (18, 26), advanced *KRAS*-mutant lung cancers are treated with conventional therapy, most often with limited success.

Because lung adenocarcinoma is so often associated with mutations in *KRAS* and *TP53*, targeted inhibition of KRAS expression and stimulation of TP53 effector functions are attractive therapeutic strategies for this disease. However, direct and specific KRAS inhibition by small-molecule compounds has been elusive (26, 27). As a result, KRAS is a promising candidate for RNAi-based therapy, which can inhibit traditionally undruggable targets by directly reducing mRNA expression. Importantly, mouse models using conditional expression of oncogenic *Ras* alleles have demonstrated that withdrawal of RAS signaling results in rapid tumor regression in established tumors (28–30). These data provide proof of principle that oncogenic RAS can play a critical role in tumor maintenance and suggest

Significance

Small RNAs can potently and precisely regulate gene expression; as a result, they have tremendous clinical potential. However, effective delivery of small RNAs to solid tumors has remained challenging. Here we report that a lipid/polymer nanoparticle can deliver small RNAs to treat autochthonous tumors in the so-called "KP" mouse model of lung cancer. Nanoparticles formulated with mimics of the p53-regulated miRNA miR-34a downregulated target genes and delayed tumor progression, while nanoparticles formulated with siRNA targeting Kirsten rat sarcoma viral oncogene homolog (siKras) slowed tumor growth and increased apoptosis. Notably, concurrent delivery of miR-34a and siKras increased anti-tumor effects, and led to tumor regression. These results demonstrate that small RNA therapies can impact solid lung tumor growth, and that targeted RNA combination therapies may be used to improve therapeutic response.

Author contributions: W.X., J.E.D., T.T., R.L., D.G.A., and T.J. designed research; W.X., J.E.D., T.T., O.F.K., S.S., A.D., W.C., L.M.C., G.R.Y., D.G.C., G.S., and A.S. performed research; W.X., J.E.D., T.T., R.B., G.S., A.S., and T.J. analyzed data; and W.X., J.E.D., T.T., D.G.A., and T.J. wrote the paper.

The authors declare no conflict of interest.

[1]W.X. and J.E.D. contributed equally to this work.

[2]To whom correspondence may be addressed. Email: dgander@mit.edu or tjacks@mit.edu.

This article contains supporting information online at www.pnas.org/lookup/suppl/doi:10.1073/pnas.1412686111/-/DCSupplemental.

that inhibiting oncogenic *RAS* with siRNA might be an effective therapy.

The *p53* tumor suppressor gene (also known as *TP53* or *Trp53*) is among the most frequently mutated genes in human cancer (31, 32); multiple tumor types exhibit a high frequency of mutation or loss of this key tumor suppressor. Restoring p53 function induces antitumor effects in multiple tumor types (reviewed in ref. 32), including lung cancer (31, 33). Despite its high frequency of involvement in human cancer, loss-of-function mutations in p53 are a challenging therapeutic target, with the possible exception of drugs that convert mutant p53 proteins to a functional state (32). The miR-34 family of miRNAs comprises direct transcriptional targets of p53 and can mediate certain effects of the p53 response (34, 35). The three members of this family, miR-34a, miR-34b, and miR-34c, have been shown to inhibit genes involved in controlling cell cycle progression, metabolism, and apoptosis (36–38). miR-34 overexpression has been shown to limit cancer cell growth and tumor progression in subcutaneous models and an autochthonous model of NSCLC, in which oncogenic *Kras* is activated without the concurrent deletion of p53 (12, 17, 35, 39). These data suggest that systematic delivery of miR-34 might be an effective strategy to stimulate the tumor suppressor pathway downstream of p53.

Although the therapeutic potential of RNA therapies is substantial, the biggest challenge in small RNA therapy remains the efficient and specific delivery to the desired target tissues (7). In vivo RNA delivery is limited by several factors, including reticuloendothelial system clearance and nuclease degradation. Nanomaterials formed with gold, silver, protein, cholesterol, DNA origami, lipids, and cationic polymers have all been investigated as potential vehicles for small RNA delivery in vivo (40). However, despite the diverse chemical and physical structures examined to date, highly efficient nonviral delivery has been largely limited to hepatocytes. For example, lipids and lipid-like materials, termed lipidoids, have reduced hepatocyte target gene expression at doses as low as 0.01 mg/kg (41, 42).

Small RNA cancer therapies are beginning to be tested in human clinical trials. Lipid nanoparticles carrying VEGF and kinesin spindle protein siRNA have been tested in phase I clinical trials in patients who have cancer with liver metastasis (43), and cyclodextrin polymer-based nanoparticles carrying ribonucleotide reductase M2 siRNA have been tested in patients with solid tumors (44). These studies have shown promising pharmacodynamics and tolerability, indicating that nanoparticle-mediated siRNA delivery may be effective in patients. However, to extend small RNA therapy to other major cancer types, including lung cancer, delivery vehicles that target nonliver tissues are urgently needed.

Recently, we reported a new class of nanoparticle-forming compounds that were generated by combinatorial chemical synthesis (45). The compounds were synthesized by conjugating epoxide-terminated lipids to low-molecular weight polyamines with an epoxide ring-opening reaction. The resulting structures were tested for their ability to complex siRNA and reduce gene expression in vitro; the most effective candidates were then tested in vivo. We identified one compound from a library of over 500 candidate delivery materials that delivered siRNA to lung endothelium in vivo, silencing target genes in pulmonary vasculature at doses several hundred-fold lower than previously reported vehicles. This compound, named 7C1, preferentially targeted lung vasculature without significantly transfecting immune cells or hepatocytes at low doses (45). These observations suggested that 7C1 might also deliver therapeutic RNA to lung cancer cells, at higher doses. Here, we describe the treatment of KP lung tumors by systemic delivery of a miR-34 mimic and siRNAs targeting Kras using 7C1 nanoparticles. Delivery of either one of these small RNAs modulated biological function in tumors and elicited antitumor effects. The concurrent delivery of both caused measurable regression of established tumors and prolonged survival of chemotherapy-treated mice. These results demonstrate that effective delivery of therapeutic small RNAs is possible in an autochthonous solid tumor model in the mouse and provide further impetus to develop small RNA-based treatment strategies for human patients with lung cancer.

Results

Delivery of siRNA to Lung Adenocarcinoma Cells in Vitro. The 7C1 compound was discovered using a combinatorial chemical engineering approach followed by cell-based and whole-animal screening (45). The 7C1 compound was synthesized by reacting 600 molecular-weight polyethyleneimine with a 15-carbon lipid tail in ethanol for 48–72 h. This chemical reaction generated a compound that, when mixed with $C_{14}PEG_{2000}$ at a 7C1/ PEG molar ratio equal to 80:20, formed nanoparticles with a multilamellar structure, a diameter of 50 nm, and a zeta potential equal to zero at physiological pH (Fig. 1*A*).

Because 7C1 allows for delivery of siRNA to pulmonary endothelial cells in vivo, we examined whether it could deliver small RNAs to lung tumor cell lines and lung tumors. We first tested 7C1-mediated siRNA delivery to KP-derived lung adenocarcinoma lines (KP cells) in vitro using fluorescence and confocal microscopy. The 7C1 nanoparticles complexed with Cy5.5 fluorophore-labeled siRNA substantially increased the intracellular Cy5.5 signal in KP cells (Fig. 1*B*). Using KP cells stably expressing firefly luciferase, we observed that 7C1 nanoparticles carrying siRNA targeting luciferase (siLuc) also reduced luminescence in a dose-dependent fashion, whereas nanoparticles carrying small interfering GFP (siGFP) had no effect (Fig. 1 *C* and *D*). Conversely, in KP cells stably expressing GFP, 7C1 nanoparticles carrying Cy5.5-siGFP simultaneously reduced GFP expression and increased Cy5.5 fluorescence (Fig. S1). Taken together, these data demonstrate 7C1 nanoparticles can deliver siRNA in cultured murine lung cancer cells.

Delivery of siRNA to Lung Adenocarcinomas in Vivo. Previous analysis has demonstrated that 7C1 is well tolerated in mice and does not induce liver enzymes (45). To assess the ability of 7C1 nanoparticles to deliver small RNAs in lung adenocarcinomas in vivo, KP mice were crossed with two strains carrying Lox-STOP-Lox reporter alleles, $R26^{LSL\text{-}tdTomato}$ and $R26^{LSL\text{-}Luciferase}$ (46, 47), to generate $Kras^{LSL\text{-}G12D/wt}$;$p53^{flox/flox}$;$R26^{LSL\text{-}Luciferase/LSL\text{-}tdTomato}$ mice. In this model, intranasal inhalation of Adeno-Cre causes deletion of p53 and activation of $Kras^{G12D}$, as well as the reporters luciferase and tdTomato, in developing lung tumors (Fig. S2*A*). Ten weeks after tumor initiation, mice were i.v. injected with a single 1.5-mg/kg dose of 7C1 nanoparticles formulated with Cy5.5-siLuc. Animals were killed at different time points, and lung tissue was isolated for confocal image analysis. To measure the luciferase signal at the single cell level, we performed immunofluorescent staining on lung tumor sections using a luciferase antibody. Tumor luciferase staining diminished 24 h after dosing, whereas tdTomato fluorescence remained constant over time, indicating that siLuc selectively silenced gene expression in tumors in vivo following i.v. injection (Fig. 1*E* and Fig. S2*B*). The 7C1 carrying siLuc also transiently reduced the luciferase signal in the lung by whole-body luciferase imaging (Fig. S2*C*). Biodistribution studies confirmed siRNA delivery to KP tumors in vivo; lung tumors isolated from mice injected with Cy5.5-labeled siRNA showed Cy5.5 fluorescence ($n = 3$ mice per group; Fig. S3). Cy5.5 signal was also distributed to kidneys and other organs (Fig. S3).

Systemic miR-34a Delivery Delays Lung Tumor Progression. We next examined whether miRNA delivery might cause therapeutic responses by restoring an effector arm of the p53 pathway to these p53-deficient tumors. As predicted by the known regulation of the miR-34 family by p53, RT-quantitative (Q)-PCR analysis

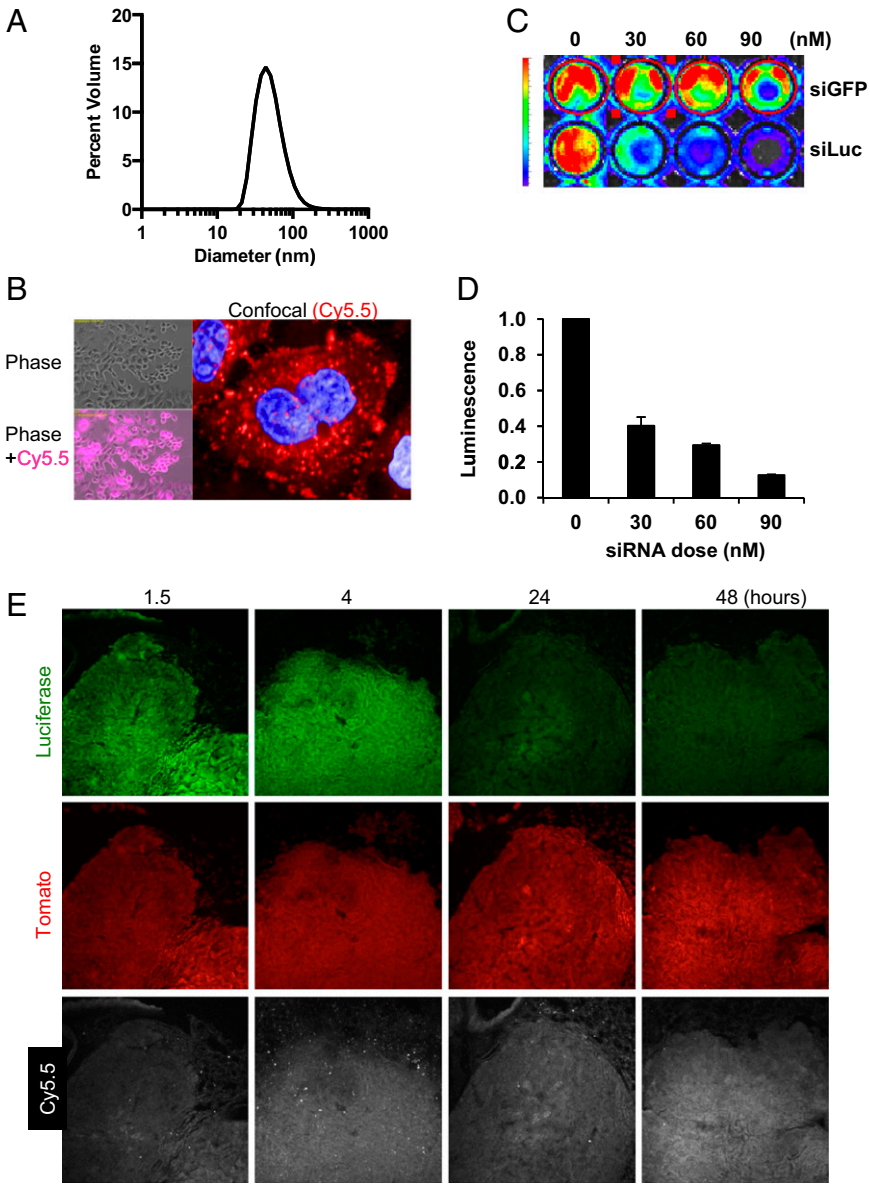

Fig. 1. Efficient delivery of siRNAs to murine lung adenocarcinoma in vitro and in vivo. (*A*) 7C1-siRNA particle diameter, weighted by volume. (*B*) Cy5.5 fluorescence in KP (*Kras*$^{LSL\text{-}G12D/wt}$;*p53*$^{flox/flox}$) cells following incubation with 7C1 nanoparticles formulated with Cy5.5-labeled siRNA at an siRNA concentration of 30 nM. Cells were washed extensively and imaged using an epifluorescence or confocal microscope, 200× and 1600× magnification, respectively. Nuclei were stained with DAPI (blue). (*C*) Firefly luminescence in KP cells following incubation with 7C1 nanoparticles carrying siLuc or siGFP (with the latter acting as a control). Representative images are shown. The color bar denotes luciferase signal intensity. (*D*) Quantification of luciferase signal in *C*. Error bars are SD ($n = 3$ wells). (*E*) 7C1 nanoparticles carrying siLuc knockdown luciferase expression in KP tumors in vivo. Lung tumors were initiated in *Kras*$^{LSL\text{-}G12D/wt}$;*p53*$^{flox/flox}$;*R26*$^{LSL\text{-}Luciferase/LSL\text{-}tdTomato}$ mice with Adeno-Cre. Ten weeks later, mice were dosed with 1.5 mg/kg of Cy5.5-siLuc formulated with 7C1, and lung tumors were harvested for luciferase immunostaining and determination of natural fluorescence of Tomato and Cy5.5. (Magnification: 400× confocal images.) Shown are representative images from seven or more tumors analyzed per time point.

showed that mature miR-34a and miR-34c were relatively underexpressed in isolated KP lung tumors compared with normal lung samples (Fig. S4). A 22-nt dsRNA, 2-O-methyl, modified to reduce immunostimulation and nuclease degradation, with the mature miR-34a antisense strand sequence and a complementary sense strand was used as the miR-34a mimic (48, 49) (Fig. S5*A*). Groups of three KP mice with established lung tumors were injected i.v. with a single 1.5-mg/kg dose of 7C1 nanoparticles complexed with siLuc, which served as a control siRNA, or the miR-34a mimic (Fig. 2*A*). Lung tumors were isolated 48 h and 68 h following injection, and miR-34a and miR-34c mature miRNAs were measured by RT-Q-PCR probes recognizing both endogenous miR-34 as well as the miRNA mimic. miR-34a increased in tumors isolated from miR-34a–treated animals compared with tumors isolated from mice treated with siLuc, whereas miR-34c levels remained constant (Fig. 2*B*). Importantly, miR-34a treatment reduced the mRNA expression of *Ccnd1*, *Sirt1*, *Cdk6*, and *Ccne2* (34), demonstrating that delivery of miR-34a achieved functional inhibition of canonical miR-34a targets in vivo (Fig. 2*C*). To optimize nanoparticle administration, groups of four KP mice were injected with the miR-34a nanoparticle formulation i.v., intranasally, or i.p. (Fig. S5*B*). The i.v. injection increased miR-34a levels in lung tumors the most, resulting in a 27-fold increase relative to mice treated with siLuc (Fig. S5*C*).

We next investigated the effects of miR-34a delivery on lung tumor development. Ten weeks after infection with Adeno-Cre, KP mice were scanned by microcomputed tomography (microCT) to measure individual tumor volumes. Tumor-bearing KP mice were i.v. injected with PBS, nanoparticles carrying siLuc, or nanoparticles carrying miR-34a at a dose of 1.5 mg/kg twice each week for 4 wk ($n = 6$ mice per group). miR-34a treatment significantly delayed tumor progression compared with siLuc and PBS control animals, which grew rapidly over this time period (Fig. 2*D*). To explore the mechanism of miR-34a in tumor suppression, lung tumors were harvested 72 h after a single i.v. injection of 1.5 mg/kg of miR-34a. Consistent with the function of miR-34a in inducing cell cycle arrest (34, 35), tumors treated with miR-34a showed reduced levels of proliferation as measured by Ki67 or phospho-histone H3 staining compared with PBS- or siLuc-treated mice (Fig. 2 *E* and *F*). Cleaved caspase 3 (CC3) staining, a marker for apoptosis, did not significantly

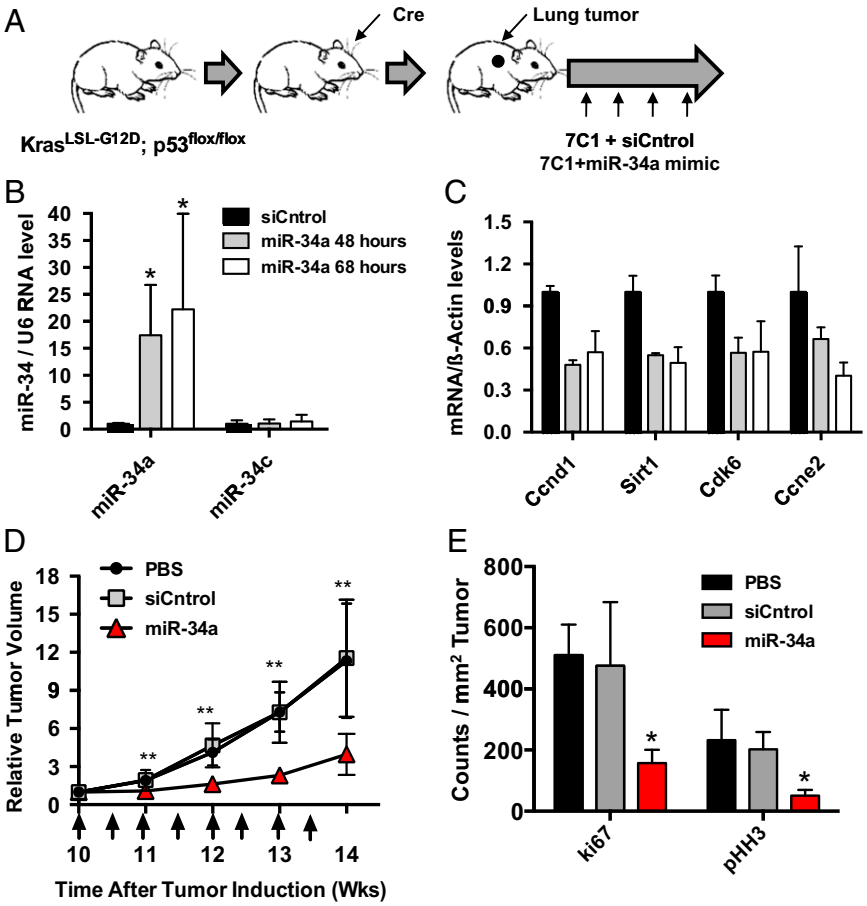

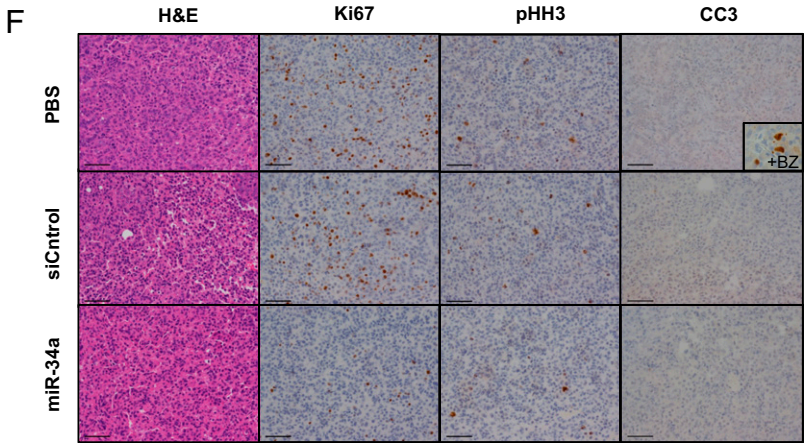

Fig. 2. Systemic miR-34a delivery delays lung tumor progression. (*A*) Experimental design. (*B*) 7C1 nanoparticles deliver miR-34a mimics to KP lung tumors. Expression levels of mature miR-34a and miR-34c in lung tumors was measured by Q-PCR 48 h and 68 h after a single injection of 1.5 mg/kg of 7C1-siLuc or 7C1–miR-34a. Error bars are SD (n = 4 tumors per group). (*C*) Expression levels of miR-34a target genes in lung tumors measured by Q-PCR. Error bars are SD (n = 3 tumors per group). *Ccnd1*, *Sirt1*, *Cdk6*, and *Ccne2* are miR-34a target genes. (*D*) Relative tumor volume measured by microCT shows a significant delay in lung tumor progression in KP mice treated with 7C1–miR-34a compared with 7C1-siLuc or PBS. Ten weeks after tumor initiation, mice were dosed with 1.5 mg/kg of siRNA or miRNA mimic twice weekly. Error bars are SD (n = 6 mice per group, n = 1 tumor per mouse). (*E*) Quantification of dividing cells marked by Ki67 and phosphohistone H3 (pHH3) in treated tumors (n = 10 tumors per group). (*F*) Representative histology and immunohistochemistry staining of lung tumors from mice treated with PBS, 7C1-siLuc, or 7C1–miR-34a. (*Inset*) Bortezomib-treated KP tumors serve as a positive control for CC3 staining. (Scale bars: 50 μm.) *P < 0.05; **P < 0.01. siCntrol, small interfering control.

increase between the three groups (Fig. 2*F*). Despite the fact that miR-34a was increased in normal lung tissue in these animals as well (Fig. S5*B*), animals treated with miR-34a showed negligible weight loss over the treatment period (Fig. S6*A*). These results provide compelling evidence that delivery of exogenous miR-34a can suppress lung tumor development in an aggressively growing autochthonous solid tumor model.

Systemic Small Interfering Kras Delivery Elicited Anti-Lung Tumor Effects. In addition to lacking p53 function, the tumors in KP mice carry an activated *Kras* oncogene, and oncogenic *Kras* is an attractive target for small RNA therapy. We screened nine siRNAs (2-O-methyl–modified) for efficient knockdown of mouse *Kras* in KP cells (Fig. S7*A*). One siRNA, si923 [hereafter termed small interfering Kras (siKras)], reduced total *Kras* mRNA expression by 87% 48 h after transfection at a 10 nM concentration compared with siLuc siRNA (Fig. S7*A*). This siKras sequence targets the 3′-UTR of *Kras* mRNA, and therefore inhibits both the oncogenic and WT *Kras*. As shown in Fig. 3*A*, incubation of KP cells with 7C1 nanoparticles carrying siKras resulted in a dose-dependent decrease in cell number and reduced phospho-Erk (pErk; p42/p44 MAPK) levels, a biomarker of Kras activity (27). To examine whether these effects were due to on-target inhibition of *Kras*, a $Kras^{G12D}$ cDNA was cloned lacking the 3′-UTR ($Kras^{G12D*}$), thus rendering it insensitive to silencing. KP cells expressing the $Kras^{G12D*}$ cDNA maintained pErk levels and showed no growth defects following exposure to siKras (Fig. 3*B* and Fig. S7*B*).

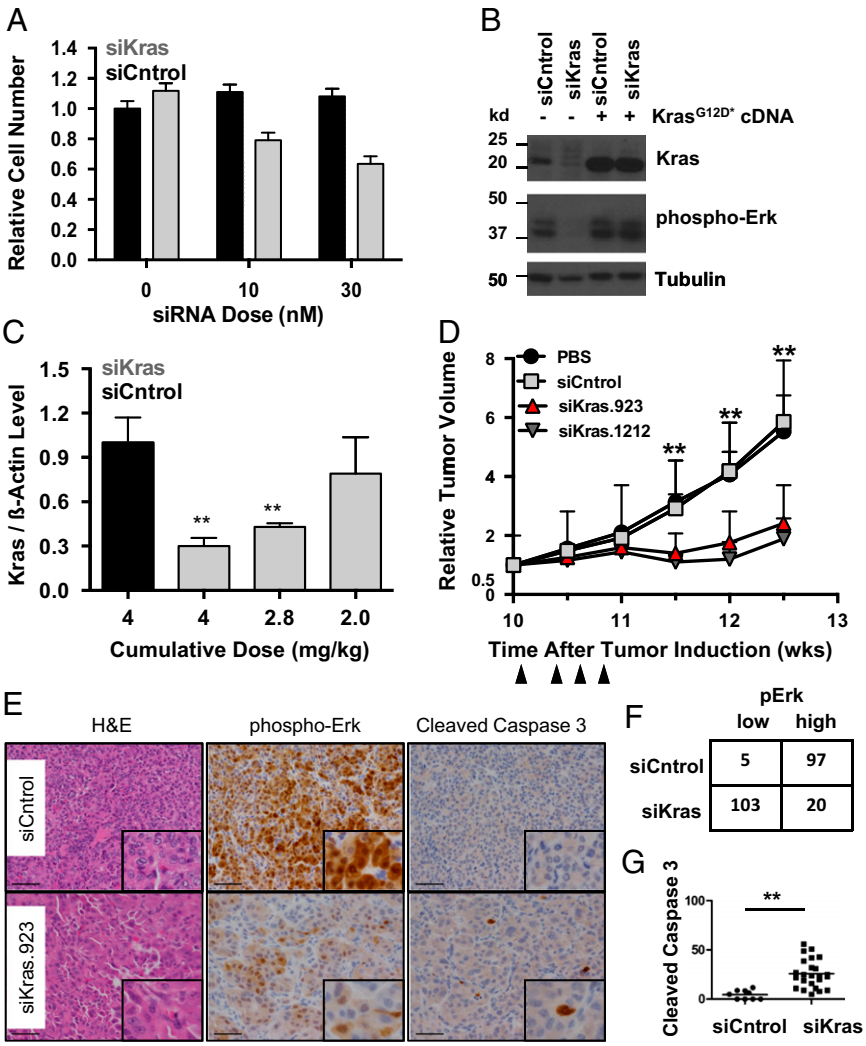

Fig. 3. Systemic siKras delivery elicited antitumor effects. (*A*) KP cell number following incubation with 7C1-siLuc or 7C1-siKras. Error bars are SD ($n = 3$ wells per group). (*B*) Immunoblots of protein lysates of KP cells expressing vector or siRNA-refractory Kras cDNA ($Kras^{G12D*}$) following incubation with 7C1-siLuc or 7C1-siKras. (*C*) Kras mRNA expression in lung tumors isolated from KP mice following injection with 7C1-siLuc or 7C1-siKras. Mice received two i.v. injections of 7C1-siRNA, and tumor RNA was harvested 72 h after the second injection. Error bars are SD ($n = 4$ mice per group, one tumor per mouse). (*D*) Relative lung tumor volume in KP mice, measured by microCT, following treatment with 7C1-siLuc or 7C1-siKras. Ten weeks after tumor initiation, mice were injected with 1.5 mg/kg of 7C1-siRNA every other day for four injections. Error bars are SD ($n = 6$ mice per group, $n = 2$ tumors per mouse). Arrowheads indicate time points of nanoparticle administration. (*E*) Representative histology and immunohistochemistry staining of lung tumors from mice treated with 7C1-siLuc or 7C1-siKras. (Scale bars: 50 μm.) (*F*) Numbers of grade 3 lung tumors with low or high levels of pErk in *E*. $P < 10^{-6}$. (*G*) Quantification of CC3-positive cells per square millimeter of tumor area in *E* ($n = 9$ and 24 tumors analyzed). $*P < 0.05$; $**P < 0.01$.

To test the effects of siKras in vivo, tumor-bearing KP mice were treated with different doses of 7C1 nanoparticle formulated with siKras or siLuc ($n = 4$ mice per group). Following two injections of 2 mg/kg, siKras treatment reduced *Kras* mRNA in isolated tumors by 63% compared with tumors treated with siLuc (Fig. 3*C*). To monitor lung tumor progression following siKras treatment, we initiated lung tumors in a cohort of KP mice. Ten weeks later, groups of six mice were injected i.v. with nanoparticles carrying 1.5 mg/kg of siKras or siLuc every other day for four doses. Individual lung tumor volumes were measured by microCT imaging over a 2.5-wk period. As shown in Fig. 3*D*, siKras-treated tumor growth was significantly inhibited compared with tumors treated with siLuc. Moreover, a modest regression was observed in some tumors (Fig. 3*D* and Fig. S7*C*). In high-grade lung tumors from siKras-treated mice, levels of pErk were markedly lower compared with control tumors (Fig. 3 *E* and *F* and Fig. S7*D*), suggesting that Kras knockdown inhibits downstream MAPK signaling. Because low-grade KP tumors do not stain positively for pErk (31), we were not able to measure the pErk levels in low-grade tumors by immunohistochemistry. To investigate mechanisms of tumor regression further, we stained lung tumor sections with an antibody specific for CC3, a marker of apoptosis. siKras-treated tumors had increased numbers of apoptotic cells compared with tumors treated with siLuc (Fig. 3 *E* and *G*). These data suggest that systemic siRNA delivery reduced oncogenic Kras mRNA in vivo and that such treatment led to antitumor responses. To confirm that these effects were due to Kras inhibition rather than off-target effects, we tested a second siRNA against *Kras* (siKras.1212). Once again, we observed down-regulation of Kras expression in vitro and antitumor effects in vivo (Fig. 3*D* and Figs. S7*A* and S8).

Concurrent Delivery of miR-34a and siKras Improves Therapeutic Responses. RNAi-based therapeutics can potentially inhibit multiple target genes and pathways via concurrent delivery of distinct small RNAs. We hypothesized that targeting activated

Kras by siRNA and stimulating p53-related responses with miR-34a would increase antitumor activity in the KP mouse model. Thus, we formulated 7C1 nanoparticles with the miR-34a mimic and siKras in an equal molar ratio. Incubation of KP cells in vitro with the miR-34a/siKras combination nanoparticles led to an additive inhibition of cell proliferation compared with miR-34a or siKras alone plus siLuc (Fig. 4*A*). To determine the therapeutic effects of combined miR-34a and siKras delivery in vivo, KP mice in which tumors were initiated 10 wk earlier were randomized into four nanoparticle treatment groups ($n = 8$ mice per group): (*i*) siLuc, (*ii*) miR-34a/siLuc, (*iii*) siKras/siLuc, and (*iv*) miR-34a/siKras. Mice were i.v. injected with a total small RNA dose of 2.0 mg/kg every other day four times. In isolated lung tumors, small RNA Q-PCR revealed increased miR-34a levels and detectable siKras antisense-strand levels in miR-34a/siKras combination-treated tumors (Fig. S9), demonstrating that nanoparticles successfully delivered both small RNAs into lung tumors. Moreover, microCT imaging revealed that miR-34a/siKras combination therapy induced measurable lung tumor regression, shrinking tumors to an average of 63% of the original volume in 2 wk (Fig. 4*B*). Combination-treated tumors also showed increased numbers of CC3-positive cells compared with miR-34a or siKras alone (Fig. 4*C*). These data suggest that effective delivery of two therapeutic small RNAs is possible in autochthonous lung tumors.

All animals tolerated small RNA therapy well, with only mild weight loss observed after siKras or miR-34a/siKras combination therapy (Fig. S6). Weight loss was not observed after injection of nanoparticles formulated with siLuc or miR-34a mimic (Fig. S6), suggesting that this effect was likely due to modulation of Kras levels in normal tissue. To examine whether tumor regression was due to a nonspecific immune response, we collected peripheral blood from animals treated with siLuc or miR-34a/siKras nanoparticles 4 h and 24 h after the first injection and 4 h after the fourth injection to monitor both acute and long-term immune responses (48, 49) (Fig. S10*A*). The dosing regimen of nanoparticles was identical to that used for tumor treatment studies (Fig. 4*B*). As measured by ELISAs, levels of IL-6 and IFN-α, indicators of nonspecific immune responses, were statistically indistinguishable in PBS-, control siRNA-, or miR-34a/siKras-treated animals at all time points (Fig. S10 *B* and *C*). Histopathological analysis showed an absence of general tissue toxicity after 7C1 miR-34a/siKras treatment (Fig. S10*D*). Collectively, these data suggest that tumor regression was not caused by an immunostimulatory effect of small RNA or nanoparticles.

Cisplatin is a first-line lung cancer chemotherapeutic agent whose efficacy has been investigated in KP mice (25). To analyze the long-term effects of nanoparticle therapy in combination with conventional chemotherapy and to examine its effect on long-term survival, we investigated whether nanoparticles

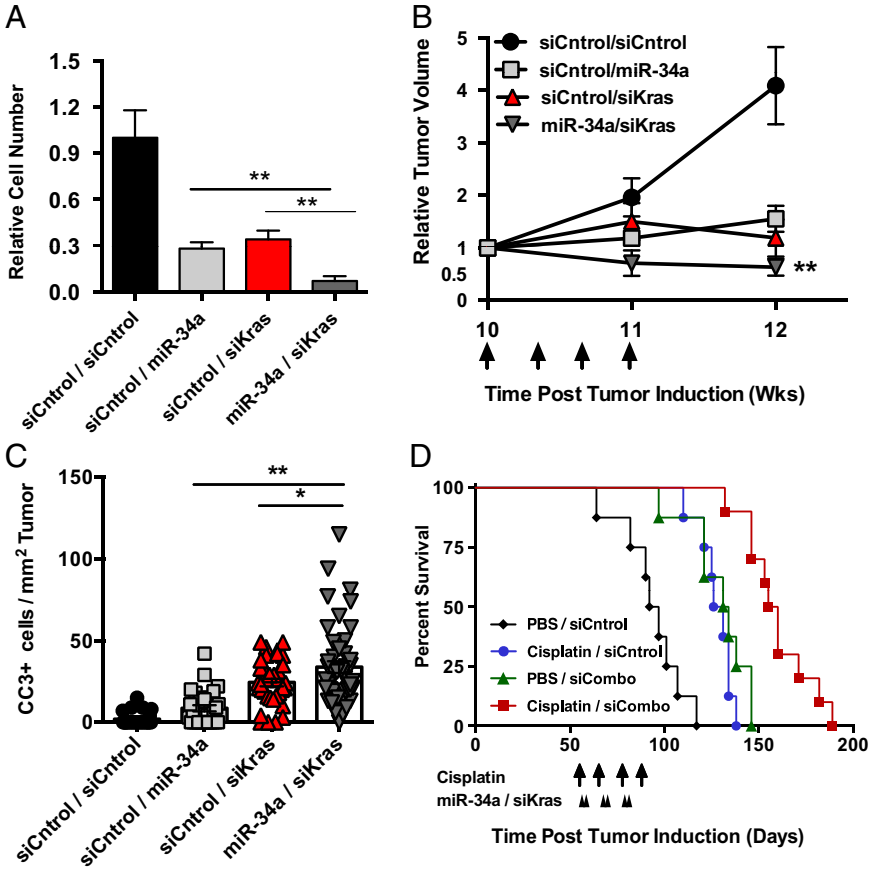

Fig. 4. Concurrent delivery of miR-34a and siKras combination improves therapeutic response. (*A*) KP cell number following incubation with 7C1-siRNA combinations. Each siRNA dose is 30 nM. Error bars are SD ($n = 3$ wells per group). (*B*) Normalized lung tumor volume in KP mice following treatment with 7C1-siRNA combinations. Ten weeks after tumor initiation, mice were dosed with 2 mg/kg of 7C1-siLuc or 7C1–miR-34a/siKras every other day for four doses. Error bars are SD ($n = 8$ mice per group, $n = 1$ tumor per mouse). $^{**}P < 0.01$ for 7C1–miR-34a/siKras compared with single treatment. (*C*) Quantification of apoptotic cells marked by CC3 in treated tumors ($n = 27$, 29, 36, and 46 tumors per time point, respectively). (*D*) Kaplan–Meier survival curve of KP mice treated with cisplatin and 7C1 nanoparticle formulated with miR34a/siKras combination (siCombo) therapies ($n = 8$, 8, 8, and 10 mice per group). Day 0 refers to tumor initiation. Arrows or arrowheads indicate time points of cisplatin or nanoparticle administration, respectively. $^{*}P < 0.05$; $^{**}P < 0.01$.

carrying miR-34a mimic and siKras could prolong life in mice separately or in combination with cisplatin. We treated tumor-bearing KP mice with either cisplatin, nanoparticles carrying both miR-34a mimic and siKras, or a combination of the two. Using the treatment regimen shown in Fig. 4*D*, KP mice treated with both cisplatin and the nanoparticle formulated with a combination of miR-34a/siKras (159.9 ± 19.5 d, $n = 10$ mice per group; $P < 0.01$ compared with single treatment) survived significantly longer than mice treated with siLuc (93.7 ± 16.1 d, $n = 8$ mice per group), cisplatin alone (127.4 ± 9.0 d, $n = 8$ mice per group), or miR-34a/siKras alone (129.2 ± 16.2 d, $n = 8$ mice per group). These data indicate that nanoparticle-mediated miR-34a/siKras small RNA therapy can provide additional therapeutic effects in combination with conventional chemotherapeutic strategies.

7C1 Carrying *KRAS* siRNA Has Therapeutic Effect in *KRAS* Mutant Human NSCLC Cells. To assess whether 7C1 can deliver therapeutic siRNA to human NSCLC cells, we formulated 7C1 nanoparticles with siRNAs targeting human *KRAS*. The 7C1 carrying siKRAS led to marked knockdown of *KRAS* mRNA in four human NSCLC cell lines harboring *KRAS* mutations and resulted in a reduced cell number (Fig. S11 *A* and *B*). The 7C1 carrying siKRAS also reduced KRAS protein in H2009 cells (Fig. S11*C*). To explore whether 7C1 formulated with siRNA targeting human *KRAS* mRNA had therapeutic efficacy in vivo, we injected *KRAS* mutant H2009 NSCLC cells s.c. into nude mice and treated mice when tumors reached 100 mm^3. Consistent with our data in the autochthonous mouse model (Fig. 3), 7C1 formulated with siKRAS delayed tumor growth of H2009 xenograft ($n = 6$ tumors per group; Fig. S11*D*). These data indicate that 7C1 nanoparticles are capable of delivering therapeutic siRNA in human NSCLC cells and xenograft tumors.

Discussion

Here, we have demonstrated that systemic delivery of a polymer-based nanoparticle can deliver therapeutic small RNAs in an autochthonous mouse model of lung cancer, and that targeted combination RNA therapy can elicit a potent antitumor response. Because a significant number of human lung tumors, as well as other tumor types, carry mutations in *KRAS* and *p53*, these results may have direct translational implications for human cancer treatment. Moreover, because 7C1 nanoparticles complex the anionic RNA backbone independent of nucleotide sequence, 7C1 can deliver therapeutic RNAs against additional targets in tumor cells. This clearly demonstrates that combination small RNA therapy is a modular and flexible approach for lung cancer treatment. Targeted multigene therapy may be used for personalized therapies because combinations can be selected against mutations identified in individual patients. As nanoparticle formulations targeted to different organs become available, synthetic siRNA or miRNA can be formulated with vehicles to target different organs of interest, potentially targeting both primary and metastatic sites.

We show here that delivery of a miR-34a mimic modulated miR-34 target genes in lung tumors and delayed tumor progression, suggesting that systematic delivery of miR-34 might be a strategy to restore partial p53 downstream functions in *TP53* mutant tumors (37). Delivery of miR-34a reduced cell proliferation and delayed lung tumor growth, which is consistent with a recent study in a $Kras^{G12D};p53^{R172H}$ lung cancer model (12). Because miR-34 family miRNAs also inhibit key signaling pathways, including NOTCH, WNT and MET (38), miR-34 may play other tumor-suppressive functions in addition to cell cycle regulation. To date, more than 30 genes targeted by miR-34a have been reported in the literature (39). Because miRNAs generally regulate large networks of target genes, miR-34a or other tumor suppressor miRNAs could be used to inhibit tumor cell proliferation and survival potently. Importantly, the inhibition of multiple target genes and pathways might limit the ability of tumor cells to escape via secondary mutations. Future work will address whether treated tumors acquire resistance to small RNA therapies through mechanisms that include reduced nanoparticle uptake, increased nanoparticle exocytosis, and global down-regulation of RNAi pathway function, and whether combination therapies designed to inhibit the expression of resistance-promoting genes simultaneously can improve therapeutic efficacy.

Although small-molecule inhibition of oncogenic Kras has not been successful to date (27), our results using Kras siRNA indicate that RNAi may effectively reduce Kras activity in vivo and induce antitumor effects (50). Because the siKras sequences in this study target the 3′-UTR of Kras, both the G12D and the WT Kras mRNA are suppressed by siKras. Future work is needed to investigate how cells respond to the knockdown of WT Kras, and whether mutant-specific forms of siKras can be developed.

Taking advantage of the ability to package multiple small RNAs in a single nanoparticle formulation (51), we demonstrated superior antitumor response with the combination of miR-34a mimic and siKras in this model system. Molecular dissection of the interaction between the miR-34a and Kras network will reveal how the miR-34a and siKras combination improves therapeutic responses. When combined with cisplatin-based chemotherapy, miR-34a/siKras delivery further extended survival, indicating RNA therapy may be combined with chemotherapy, radiation, or surgery to improve the efficacy of existing cancer therapies. More specifically, the response to chemotherapy might be improved by specifically modulating genes in chemoresistance pathways. For example, murine lung adenocarcinoma resistant to cisplatin treatment often has elevated expression of the apoptosis modulator *Pidd* (25). Similarly, *MET* tyrosine kinase amplification has been identified in some EGFR inhibitor-resistant lung cancers (52).

Given that 7C1 nanoparticles are known to target endothelial cells, additional studies are required to delineate the impact of siKras and miR-34a delivery on normal tissue and the tumor microenvironment. However, it is clear that these small RNAs had direct effects on the tumor cells as well, as evidenced by knockdown of a tumor cell-specific luciferase reporter in vivo (Fig. 1*E*).

Taken together, our findings demonstrate the feasibility of small RNA-based combination therapy in a physiologically relevant mouse model of human lung cancer. The effective delivery of small RNAs to solid tumors in the model, combined with the modulation of divergent aspects of tumor biology as well as potent therapeutic responses, provides a compelling case for the use of small RNA therapies in human patients with lung cancer.

Materials and Methods

7C1 Nanoparticle Formulation. The 7C1 compound was synthesized and purified as previously described (45). Particles were formulated with a microfluidic device (53) at a 7C1/RNA mass ratio equal to 5:1, dialyzed into 1× PBS, filtered with a sterile 0.2-μm filter under a sterile biohood, and stored at 4 °C. Particle diameter was measured with a Malvern Zetasizer (Malvern Instruments).

Mice and 7C1 Nanoparticle Treatment. All animal study protocols were approved by the Massachusetts Institute of Technology Animal Care and Use Committee. Cohorts of KP and KP;$R26^{LSL\text{-}Luciferase/LSL\text{-}tdTomato}$ mice were infected with 2.5×10^7 pfu of Adeno-Cre (University of Iowa) by intranasal inhalation as described previously. Mice were injected with 7C1 nanoparticles i.v. and with cisplatin i.p. (25) as indicated. A total of 5×10^6 H2009 cells were injected s.c. in immunocompromised mice (6–8 wk old). Tumor volume was measured by calipers and calculated as 0.52 × length × $width^2$. Upon tumor formation (~100 mm^3), mice were treated with PBS or 7C1 siRNA as indicated.

Immunohistochemistry. Mice were killed by carbon dioxide asphyxiation. Lungs were inflated with 4% formalin [neutral buffered formalin (vol/vol)], fixed overnight, and transferred to 70% ethanol. Lung lobes were embedded in paraffin, sectioned at 4 μm, and stained with H&E for tumor pathology. Lung tumor sections were dewaxed, rehydrated, and stained using standard immunohistochemistry protocols (22). The following antibodies were used: anti-cleaved caspase 3 (1:200, catalog no. 9661; Cell Signaling), anti-Ki67 (1:100, VP-K452; Vector Laboratory), anti-Phospho Histone H3 (1:200, catalog no. 9701; Cell Signaling), and anti-pErk Thr202/Tyr204 (1:300, catalog no. 4370; Cell Signaling). The number of positive cells per tumor area was quantified. Tumor numbers and mice numbers are indicated in the figure legends.

MicroCT and Bioluminescence Imaging. At indicated time points, mice were scanned for 5 min under isoflurane anesthesia using small animal microcomputed tomography (eXplore CT120 whole-mouse microCT; GE Healthcare). Images were acquired and processed using GE eXplore software. One or two independent lung tumors from each mouse were quantified. Bioluminescence imaging was performed as previously described (22). Signals in mice or cells were quantified using Living Imaging software (Xenogen).

Immunoblotting, ELISA, and Immunofluorescence. Cell pellets were lysed in Laemmli buffer. Equal amounts of protein (16 μg) were separated on 10% SDS-polyacrylamide gels and transferred to PVDF membranes. Blots were probed with antibodies (1:1,000 dilution) against Kras (sc-30), pErk (catalog no. 4370; Cell Signaling), or tubulin. Serum cytokine concentrations were measured in an ELISA-based assay according to the manufacturer's instructions (eBiosciences). Immunofluorescence testing was performed as previously described (54). Goat antiluciferase (G7451; Promega) and donkey anti-goat Alexa Fluor 488 (Invitrogen) antibodies were used. Slides were counterstained with DAPI (Sigma) and mounted in Vectashield antifade mountant (Vector Laboratories).

Cell Number Measurement. Cells were split into 96-well plates (1,000 cells per well). After 24 h, cells were coincubated with 7C1 nanoparticles for 24 h. After 48–72 h, cell number was measure in triplicate using a CellTiter-Glo kit (Promega). Control siRNA-treated cell values were set to 1 (100%). For Figs. 1*D*, 3*A*, and 4*A* and Fig. S11, the data are representative of two independent experiments.

Gene Expression Analysis and Small RNA Q-PCR. RNA was purified using TRIzol (Invitrogen) and reverse-transcribed using a High-Capacity cDNA Reverse Transcription Kit (Applied Biosystems). Real-time PCR (Q-PCR) reactions were performed using Taqman probes (Applied Biosystems). mRNA levels were normalized to *Actin* mRNA. For measuring miRNA expression, 10 ng of total RNA was reverse-transcribed using miRNA-specific RT primer and measured by real-time PCR using miRNA-specific probes (Applied Biosystems). siKras levels were quantified similarly using a customized small RNA Taqman assay (Applied Biosystems). Data were normalized to the U6 RNA.

Sequence of Kras siRNAs (Antisense 5′–3′)

4504 AUGACCAACAUUCCCUAGG 2606 UAGUUUAAAUCCCACUAUG
1442 UACUAUUUCAUACUGGGUCUG1212 UAAAGUCUAGGACACGCUG
923 CUUAGAAAAAAGAAGGUUUCC745 AUUCACAUAACUGUACACC
593 AAUCCCGUAACUCCUUGCU562 UGUUUCGUGUCUACUGUUC
218 UACGCCACCAGCUCCAACC–scramble siRNA for 923 GCCUAAUAAU-AAGGAAUACGU

ON-TARGET plus Human KRAS SMART pool was purchased from Dharmacon. All siRNAs have dTdT overhang in the 3′-end.

Statistics. *P* values were determined by Prism 5 (GraphPad) and Student *t* tests.

ACKNOWLEDGMENTS. We thank D. McFadden, T. Papagiannakopoulos, N. Joshi, N. Dimitrova, E. Snyder, A. Farago, M. Muzumdar, R. Bogorad, M. Goldberg, J. Lo, S. Bhatia, D. Bumcrot, and P. Sharp for discussions and for sharing reagents; A. Deconinck, D. Feldser, and V. Gocheva for critical reading of the manuscript; S. Malstrom and M. Cornwall-Brady for animal imaging; T. Yuan, C. Fellmann, and F. McCormick for sharing the siKRAS sequence; and the entire staff of the laboratories of T.J. and D.G.A. for discussions. We thank the Swanson Biotechnology Center for technical support. This work was supported by Grants 2-PO1-CA42063, RO1-EB000244, RO1-CA115527, and RO1-CA132091 from the National Institutes of Health and supported, in part, by Cancer Center Support (core) Grant P30-CA14051 from the National Cancer Institute. T.J. is a Howard Hughes Investigator, the David H. Koch Professor of Biology, and a Daniel K. Ludwig Scholar. W.X. was supported by fellowships from the American Association for Cancer Research and the Leukemia Lymphoma Society and is currently supported by Grant 1K99CA169512. J.E.D. receives support from the National Defense Science and Engineering Graduate, National Science Foundation Graduate Research Fellowship Program, and the Massachusetts Institute of Technology Presidential Fellowships.

1. Ambros V (2008) The evolution of our thinking about microRNAs. *Nat Med* 14(10): 1036–1040.
2. Mendell JT, Olson EN (2012) MicroRNAs in stress signaling and human disease. *Cell* 148(6):1172–1187.
3. Ventura A, Jacks T (2009) MicroRNAs and cancer: Short RNAs go a long way. *Cell* 136(4):586–591.
4. Croce CM (2009) Causes and consequences of microRNA dysregulation in cancer. *Nat Rev Genet* 10(10):704–714.
5. Kasinski AL, Slack FJ (2011) Epigenetics and genetics. MicroRNAs en route to the clinic: Progress in validating and targeting microRNAs for cancer therapy. *Nat Rev Cancer* 11(12):849–864.
6. Pecot CV, Calin GA, Coleman RL, Lopez-Berestein G, Sood AK (2011) RNA interference in the clinic: Challenges and future directions. *Nat Rev Cancer* 11(1):59–67.
7. Bumcrot D, Manoharan M, Koteliansky V, Sah DW (2006) RNAi therapeutics: A potential new class of pharmaceutical drugs. *Nat Chem Biol* 2(12):711–719.
8. Kanasty RL, Whitehead KA, Vegas AJ, Anderson DG (2012) Action and reaction: The biological response to siRNA and its delivery vehicles. *Mol Ther* 20(3):513–524.
9. Whitehead KA, Langer R, Anderson DG (2009) Knocking down barriers: Advances in siRNA delivery. *Nat Rev Drug Discov* 8(2):129–138.
10. Schroeder A, et al. (2012) Treating metastatic cancer with nanotechnology. *Nat Rev Cancer* 12(1):39–50.
11. Kota J, et al. (2009) Therapeutic microRNA delivery suppresses tumorigenesis in a murine liver cancer model. *Cell* 137(6):1005–1017.
12. Kasinski AL, Slack FJ (2012) miRNA-34 prevents cancer initiation and progression in a therapeutically resistant K-ras and p53-induced mouse model of lung adenocarcinoma. *Cancer Res* 72(21):5576–5587.
13. Kanasty R, Dorkin JR, Vegas A, Anderson D (2013) Delivery materials for siRNA therapeutics. *Nat Mater* 12(11):967–977.
14. Ren Y, et al. (2012) Targeted tumor-penetrating siRNA nanocomplexes for credentialing the ovarian cancer oncogene ID4. *Sci Transl Med* 4(147):147ra112.
15. Yao YD, et al. (2012) Targeted delivery of PLK1-siRNA by ScFv suppresses Her2+ breast cancer growth and metastasis. *Sci Transl Med* 4(130):130ra148.
16. Huang YH, et al. (2009) Claudin-3 gene silencing with siRNA suppresses ovarian tumor growth and metastasis. *Proc Natl Acad Sci USA* 106(9):3426–3430.
17. Trang P, et al. (2011) Systemic delivery of tumor suppressor microRNA mimics using a neutral lipid emulsion inhibits lung tumors in mice. *Mol Ther* 19(6):1116–1122.
18. Herbst RS, Heymach JV, Lippman SM (2008) Lung cancer. *N Engl J Med* 359(13): 1367–1380.
19. DuPage M, Dooley AL, Jacks T (2009) Conditional mouse lung cancer models using adenoviral or lentiviral delivery of Cre recombinase. *Nat Protoc* 4(7):1064–1072.
20. Engelman JA, et al. (2008) Effective use of PI3K and MEK inhibitors to treat mutant Kras G12D and PIK3CA H1047R murine lung cancers. *Nat Med* 14(12):1351–1356.
21. Trejo CL, Juan J, Vicent S, Sweet-Cordero A, McMahon M (2012) MEK1/2 inhibition elicits regression of autochthonous lung tumors induced by KRASG12D or BRAFV600E. *Cancer Res* 72(12):3048–3059.
22. Xue W, et al. (2011) Response and resistance to NF-κB inhibitors in mouse models of lung adenocarcinoma. *Cancer Discov* 1(3):236–247.
23. De Raedt T, et al. (2011) Exploiting cancer cell vulnerabilities to develop a combination therapy for ras-driven tumors. *Cancer Cell* 20(3):400–413.
24. Chen Z, et al. (2012) A murine lung cancer co-clinical trial identifies genetic modifiers of therapeutic response. *Nature* 483(7391):613–617.
25. Oliver TG, et al. (2010) Chronic cisplatin treatment promotes enhanced damage repair and tumor progression in a mouse model of lung cancer. *Genes Dev* 24(8):837–852.
26. Heist RS, Engelman JA (2012) SnapShot: Non-small cell lung cancer. *Cancer Cell* 21(3): 448–e442.
27. Pylayeva-Gupta Y, Grabocka E, Bar-Sagi D (2011) RAS oncogenes: Weaving a tumorigenic web. *Nat Rev Cancer* 11(11):761–774.
28. Chin L, et al. (1999) Essential role for oncogenic Ras in tumour maintenance. *Nature* 400(6743):468–472.
29. Fisher GH, et al. (2001) Induction and apoptotic regression of lung adenocarcinomas by regulation of a K-Ras transgene in the presence and absence of tumor suppressor genes. *Genes Dev* 15(24):3249–3262.
30. Jechlinger M, Podsypanina K, Varmus H (2009) Regulation of transgenes in three-dimensional cultures of primary mouse mammary cells demonstrates oncogene dependence and identifies cells that survive deinduction. *Genes Dev* 23(14):1677–1688.
31. Feldser DM, et al. (2010) Stage-specific sensitivity to p53 restoration during lung cancer progression. *Nature* 468(7323):572–575.
32. Levine AJ, Oren M (2009) The first 30 years of p53: Growing ever more complex. *Nat Rev Cancer* 9(10):749–758.

33. Junttila MR, et al. (2010) Selective activation of p53-mediated tumour suppression in high-grade tumours. *Nature* 468(7323):567–571.
34. He L, He X, Lowe SW, Hannon GJ (2007) microRNAs join the p53 network—Another piece in the tumour-suppression puzzle. *Nat Rev Cancer* 7(11):819–822.
35. Hermeking H (2010) The miR-34 family in cancer and apoptosis. *Cell Death Differ* 17(2):193–199.
36. Hermeking H (2012) MicroRNAs in the p53 network: Micromanagement of tumour suppression. *Nat Rev Cancer* 12(9):613–626.
37. He L, et al. (2007) A microRNA component of the p53 tumour suppressor network. *Nature* 447(7148):1130–1134.
38. He X, He L, Hannon GJ (2007) The guardian's little helper: MicroRNAs in the p53 tumor suppressor network. *Cancer Res* 67(23):11099–11101.
39. Bader AG (2012) miR-34—A microRNA replacement therapy is headed to the clinic. *Front Genet* 3:120.
40. Peer D, et al. (2007) Nanocarriers as an emerging platform for cancer therapy. *Nat Nanotechnol* 2(12):751–760.
41. Semple SC, et al. (2010) Rational design of cationic lipids for siRNA delivery. *Nat Biotechnol* 28(2):172–176.
42. Love KT, et al. (2010) Lipid-like materials for low-dose, in vivo gene silencing. *Proc Natl Acad Sci USA* 107(5):1864–1869.
43. Tabernero J, et al. (2013) First-in-humans trial of an RNA interference therapeutic targeting VEGF and KSP in cancer patients with liver involvement. *Cancer Discov* 3(4):406–417.
44. Davis ME, et al. (2010) Evidence of RNAi in humans from systemically administered siRNA via targeted nanoparticles. *Nature* 464(7291):1067–1070.
45. Dahlman JE, et al. (2014) In vivo endothelial siRNA delivery using polymeric nanoparticles with low molecular weight. *Nat Nanotechnol*, 10.1038/nnano.2014.84.
46. Madisen L, et al. (2010) A robust and high-throughput Cre reporting and characterization system for the whole mouse brain. *Nat Neurosci* 13(1):133–140.
47. Cheung AF, Dupage MJ, Dong HK, Chen J, Jacks T (2008) Regulated expression of a tumor-associated antigen reveals multiple levels of T-cell tolerance in a mouse model of lung cancer. *Cancer Res* 68(22):9459–9468.
48. Whitehead K, Dahlman JE, Langer RS, Anderson DG (2010) Silencing or stimulation? siRNA delivery and the immune system. *Annu Rev Chem Biomol Eng* 2:77–96.
49. Robbins M, Judge A, MacLachlan I (2009) siRNA and innate immunity. *Oligonucleotides* 19(2):89–102.
50. Zorde Khvalevsky E, et al. (2013) Mutant KRAS is a druggable target for pancreatic cancer. *Proc Natl Acad Sci USA* 110(51):20723–20728.
51. Nishimura M, et al. (2013) Therapeutic synergy between microRNA and siRNA in ovarian cancer treatment. *Cancer Discov* 3(11):1302–1315.
52. Engelman JA, et al. (2007) MET amplification leads to gefitinib resistance in lung cancer by activating ERBB3 signaling. *Science* 316(5827):1039–1043.
53. Chen D, et al. (2012) Rapid discovery of potent siRNA-containing lipid nanoparticles enabled by controlled microfluidic formulation. *J Am Chem Soc* 134(16):6948–6951.
54. Tammela T, et al. (2011) VEGFR-3 controls tip to stalk conversion at vessel fusion sites by reinforcing Notch signalling. *Nat Cell Biol* 13(10):1202–1213.